The Effects of Winds and Photoionization on the Evolution of Protostellar Disks

Harold W. Yorke[1] and Sabine Richling[2]

[1]Jet Propulsion Laboratory, California Institute of Technology, Pasadena, CA, USA
[2]Institut für Theoretische Astrophysik, Universität Heidelberg, Germany

Introduction

The evolution and appearance of circumstellar disks in star forming regions can be influenced strongly by the radiation from nearby hot stars. UV radiation heats the outer layers of the disk and induce expansion up to escape velocities. Hollenbach et al. (2000, PPIV, 401) identify this "photoevaporation" process as a principal, if not the most important, disk destruction mechanism. Here, we describe the results of numerical simulations of the evolution of protostellar disks and their immediate surroundings under the influence of external UV radiation. In order to assess the role of central stellar winds, we have included the effects of an isotropic wind in the numerical models.

Physical Model and Numerical Methods

Using the 2D (axial symmetry assumed) radiation hydrodynamic code *EXTERN* (see Fig. 1) described in detail by Richling & Yorke (2000, ApJ, 539, 258), we calculate the evolution of externally UV-irradiated protostellar disks with the added influence of a strong (case S) and a weak (case W) isotropic wind from the disk's central star.

Table: Model Parameters

case	initial model	$\alpha_{\rm vis}$	$Z_{\rm star}$ [pc]	log $S_{\rm EUV}$ [s^{-1}]	log $S_{\rm FUV}$ [s^{-1}]	$v_{\rm wind}$ [km s^{-1}]	$\dot{M}_{\rm wind}$ [M$_\odot$ yr^{-1}]
W	YB[1]	0.01	1	48.86	49.25	5	10^{-7}
S	W[2]	0.01	1	48.86	49.25	50	2×10^{-7}

[1]The initial disk model was taken from Yorke & Bodenheimer (1999, ApJ 525, 330: The 2 M$_\odot$ case at $t = 240000$ yr produced a star of 1 M$_\odot$ with a disk of 0.5 M$_\odot$).
[2]The results of case W at $t = 100000$ yr were used.

Results and Conclusions

The UV-irradiation of the disk results in dissociation of H_2 and CO as well as heating of the outer disk layers. This warm material is no longer gravitationally bound to the disk at disk radii where the sound speed exceeds the escape velocity, and a neutral "photoevaporation" flow results. The disk and the outflow is surrounded by a teardrop shaped ionization front. A shock front is located between the disk and the I-front. During its photoevaporation the disk decreases in size and mass.
An initially isotropic stellar wind is collimated by the disk's neutral outflow into a

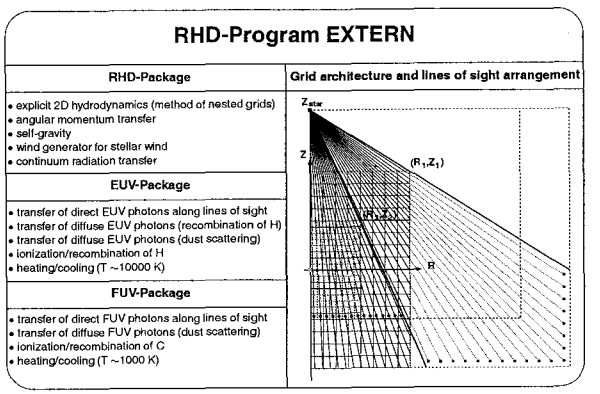

Fig. 1: Overview of the RHD program *EXTERN*. **Left:** Physical processes modeled by the code. **Right:** Example of a grid setup for two 8×16 nested grids (We used six 58×116 grids for the simulations discussed here). The external UV source is located on the symmetry axis at a distance $Z_{\rm star}$ above the equatorial plane. The disk's central star (green dot) is located at $(R, Z) = (0, 0)$. The lines of sight (black lines) used for the transfer of direct FUV and EUV photons are chosen so that each grid cell is traversed at least once.

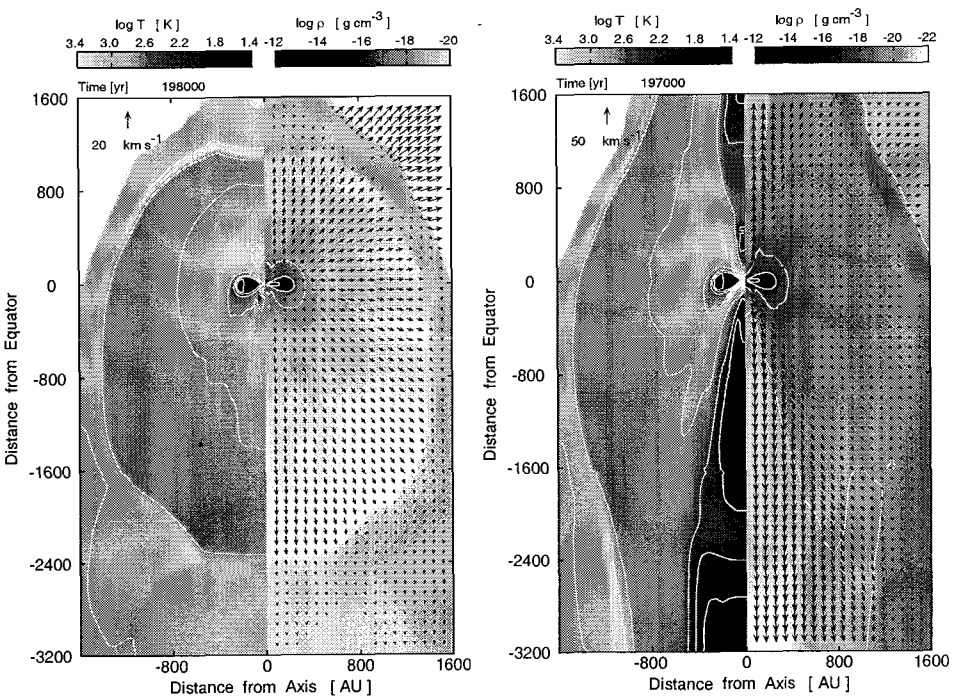

Fig. 2: Temperature (red), density (blue), and velocity (arrows) structure of photoevaporating disks. The temperature

An initially isotropic stellar wind is collimated by the disk's neutral outflow into a bipolar outflow. Because there is some degree of mixing of stellar wind (with no angular momentum) with disk material (rotating at Keplerian velocity) at the disk's inner edge, the collimated outflow contains angular momentum. As this "loaded" material moves to ever larger distances from the star, centrifugal forces cause it to expand in the radial direction. The net result is that the outflow lies in a conical shell; very little material is present inside this shell close to the rotation axis and what little is there has a very low temperature.

Because of the focusing of the stellar wind away from the disk, it had little affect on the disk itself (Fig. 2 and Fig. 3). Although the radio continuum emission (Fig. 4) does show evidence for the existence of a jet, the spectral energy distribution (Fig. 5) and the rate at which the disk is destroyed by UV irradiation (Fig. 6) were hardly affected.

Acknowledgements This research has been conducted at the Jet Propulsion Laboratory and is supported by NASA through grant NRA-99-01-ATP-065 and by the DFG (Deutsche Forschungsgemeinschaft).

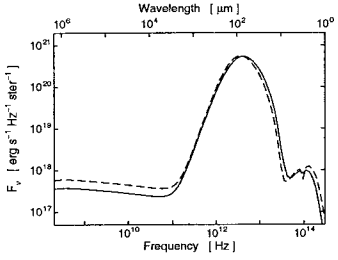

Fig. 4: Spectral energy distributions of case W (*solid line*) and case S (*dashed line*) computed for the time shown in Figs. 2 and 3.

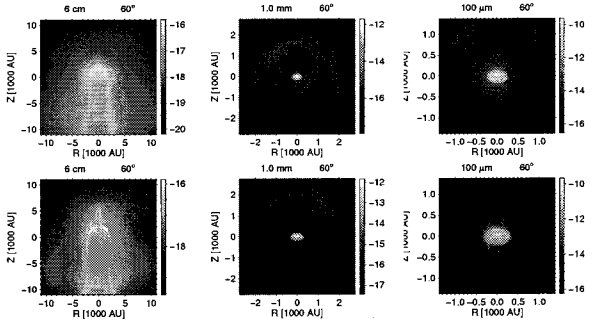

Fig. 5: Selected maps for case W (*top frames*) and case S (*bottom frames*) computed for the time shown in Figs. 2 and 3.

Fig. 2: Temperature (red), density (blue), and velocity (arrows) structure of photoevaporating disks. The temperature scale has been truncated at $\log T = 3.4$ to emphasize the shock fronts. The density and velocity scales in the left frame (case W, weak wind) and right frame (case S, strong wind) are different, but the density contour lines at $\log \rho = -20$, -18, -16, -14, and -12 are the same.

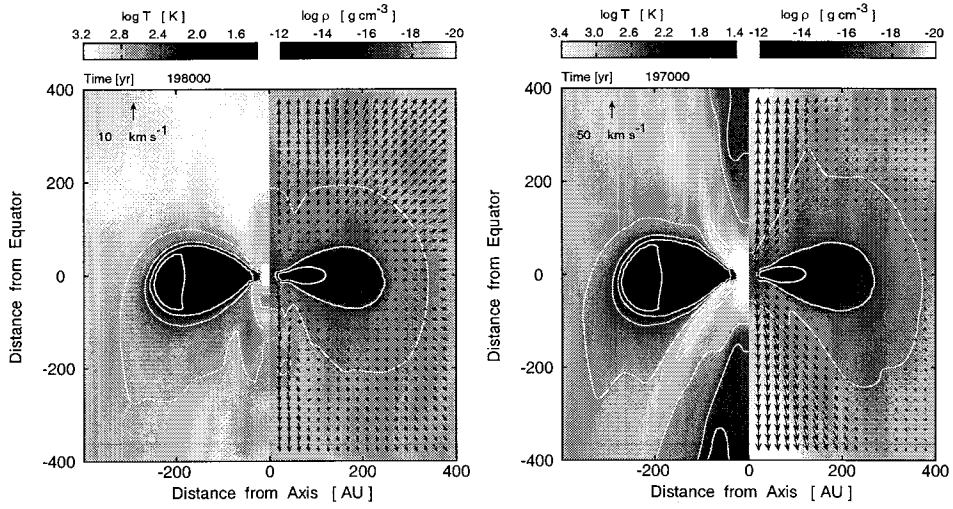

Fig. 3: More detailed view of the disk structure for the two cases considered.

Fig. 6: Evolution of masses and sizes for both case W *solid lines* and case S (*dotted lines*) **Left:** Molecular, atomic, and ionized masses within the computational grid **Right:** Z_{head} and Z_{tail} are the locations of the top and bottom of the hydrogen ionization front along the symmetry axis and R_{head} is its radial extent at $Z = 0$. R_C is the radial extent of the C-ionization front at $Z = 0$ and defines the radius of the disk.